

Original Article

# Study on Material Removal Rate in EDM Of 9XC Steel

Vinh-Binh Bui<sup>1</sup>, Xuan-Thao Dang<sup>2</sup>, Hong-Son Nguyen<sup>2</sup>, Nhu-Uyen Vo Thi<sup>1</sup>

<sup>1</sup>School of Mechanical & Automotive Engineering, Hanoi University of Industry, Hanoi City, Vietnam.

<sup>2</sup>HaUI Institute of Technology, Hanoi University of Industry, Hanoi City, Vietnam.

<sup>1</sup>Corresponding Author : binh.bui01@hau.edu.vn

Received: 18 January 2026

Revised: 27 February 2026

Accepted: 26 March 2026

Published: 29 April 2026

**Abstract** - The present work examines the effects of discharge current ( $I_e$ ) and ignition voltage ( $U_z$ ) on the rate of material removal (MRR, denoted as  $Q$ ) during EDM of 9XC alloy tool steel, a very high-hardness tool steel used for mould manufacturing. In this article, a  $2^2$  full factorial design was used to systematically study the effects of process variables on a CM 323C EDM machine. The tests were conducted on two parameters: ignition voltage (40–70V) and discharge current (2–8A); data processing was performed using MATLAB software. The results show that both are linear with MRR, but this implies that the discharge current has a much more dominant effect than the ignition voltage. In particular, an exponential regression model was formulated  $Q = 0.213 \cdot U_z^{0.432} \cdot I_e^{1.005}$ , which yielded a high Coefficient of Determination ( $R^2$ ) of 0.944 when compared with the experimental results. The proposed model establishes a sound scientific foundation for determining optimal machining parameters to improve the productivity and quality of industrial EDM of alloy tool steels.

**Keywords** - Electrical Discharge Machining, 9XC alloy steel, Material Removal Rate, Design of Experiments, Response Surface Method.

## 1. Introduction

In today's mechanical machining industry, the use of advanced materials with high temperature resistance and hardness is commonplace. To address this, Electrical Discharge Machining (EDM) has been developed and widely applied as a standard non-traditional machining solution for conductive materials, regardless of their hardness or strength [1-3].

Instead of the physical cutting force employed in mechanical processes, the mechanism of material removal in EDM is thermoelectric energy generated by a series of high-frequency discharges between the tool electrode and the workpiece in an insulating fluid medium [4]. Because this process does not require direct contact between the tool and the workpiece, EDM eliminates the problems associated with mechanical stress, vibration, and chatter commonly encountered when machining difficult-to-cut materials. The technology has critical applications in the mold-making, aerospace, and automotive parts manufacturing industries [5].

Furthermore, in the global trend towards sustainable manufacturing, research to optimize EDM processes is crucial to minimize energy consumption, reduce specific operating costs associated with long machining cycles, and minimize environmental impact from producing toxic dielectrics. To better analyze the current state of machining technology, the industrial importance and application of 9XC tool alloy steel

stems from its widespread use in the production of cold stamping dies, drill bits, and precision cutting tools. The requirement for extremely high post-hardening hardness (52-54 HRC) makes conventional machining less economically feasible [6]. Even though EDM can process these hardened materials without mechanical contact, using incorrect input parameters can result in adverse effects such as reduced Material Removal Rates (MRR) and severe electrode wear phenomenon, clearly demonstrating the need for precise optimization of electrical parameters [7].

Globally, when addressing these complexities to maximize machining performance, researchers have widely used a range of statistical and mathematical techniques. The Taguchi method, closely combined with Analysis of Variance (ANOVA), has been widely applied in many studies to identify the most important electrical factors affecting machining results [8].

In addition, Response Surface Method (RSM) has also been successfully used in many studies to build empirical regression models [9], and Multi-Criteria Decision Making (MCDM) methods have provided systematic guidance for selecting appropriate machining parameters [10]. Recent comprehensive reviews and empirical studies have also highlighted the leading role of specific electrical parameters in EDM performance. Studies by Deepa Singh et al. [11] and Pendokhare et al. [12] have established important contents on



the physical effects of discharge current on MRR and surface roughness on different tool steels.

Although traditional EDM machining is the foundation of high-hardness alloy machining, much research has incorporated new technological advancements, focusing on improving physical properties to overcome inherent limitations in debris removal and heat dissipation. New techniques such as Powder-Mixed Electrical Discharge Machining (PMEDM) and Ultrasonically Assisted Electrical Discharge Machining (UAEDM) have proven to be advanced and highly efficient machining solutions [8], [13]. PMEDM significantly reduces the voltage required to break down and widen the gap of the discharge spark [14], while UAEDM is set to introduce high-frequency mechanical vibrations and create strong acoustic cavitation, significantly improving debris removal [5], leading to enhanced overall machining performance, such as higher MRR and better surface quality [13-15]. Despite demonstrating superiority in maximizing productivity, these advanced hybrid systems create an extremely complex and difficult-to-control multidimensional variable interaction matrix [16]. Thus, when power processing complex tooling design sizes into industrial production, the machinist must have a precise mathematical concept for the manipulation of certain electrical parameters which interact with particular hard substances like 9XC steel in order to know he is making the correct adjustments.

In recent years, the trend toward optimizing non-traditional machining processes has increasingly relied on complex algorithms such as Artificial Neural Networks (ANN) or the development of evolutionary algorithms (NSGA-II) [17, 18]. At the same time, a significant research gap remains: although such advanced methods based on such data offer high accuracy, they often operate as “black boxes,” requiring specialized research software, high programming expertise, and significant computational resources. This creates a clear shortage of explicit, operator-friendly mathematical tools for estimating machining productivity in the workshop. Therefore, the novelty of this research lies in the construction of an explicit, direct, transparent, and highly reliable empirical exponential regression model specifically designed for 9XC steel in EDM machining. This model bridges the gap between sophisticated AI-based optimization tools and the practical need for rapid, high-precision machining productivity estimation in the industrial mold-making industry.

To overcome these limits and provide a firm foundation for process improvement, the current work uses a  $2^2$  full factorial design [19] to analyze the machinability of 9XC alloy tool steel on a CM 323C machine. The aim is to identify a rule governing the influence of ignition voltage and discharge current on the Material Removal Rate ( $Q$ ). Based on the experimental results, the present study seeks to establish a solid mathematical regression model in the form of an

exponential function ( $Q = a \cdot U_z^b \cdot I_e^c$ ) for predicting machining productivity. Additionally, the results will provide quantitative confirmation of the supremacy of discharge current over ignition voltage [20], thereby providing a proven scientific basis for determining the optimal cutting regimes to improve productivity in practical industry applications.

## 2. Objects, Scope, and Research Methodology

### 2.1. Research Objects

**Workpiece Material:** The samples for this experimental study were made of 9XC alloy tool steel with a cylindrical shape of  $\text{Ø}25 \times 10$  mm. These samples were heat-treated before machining to have a hardness of 52–54 HRC. This particular variety of low-alloy tool steel is known for its high hardness, high compressive strength, and superior wear resistance. It is regarded as essential for the production of cutting tools (including drills and taps) and cold-working dies.

In the novelty processing machinery (research on unconventional machining) type, 9XC shares many common metallurgical characteristics with 9CrSi (or 90CrSi) steel, which is well known in EDM research for improving EDM performance. For example, the SFM of 9CrSi steel has been studied, and recent work has focused on determining optimal input parameters for 90CrSi steel using a multi-criteria decision-making method [21]. Therefore, the choice of 9XC for the present investigation is of practical importance, as the high hardness attained by this material after quenching makes it very difficult to process with conventional cutting methods, and EDM is necessary to maintain dimensional accuracy and machining efficiency.

### 2.2. Research Scope

**Selection of Input Parameters:** The study is limited to two basic electrical quantities: the ignition voltage and the discharge current ( $I_e$ ). This choice is based on the fact that these two quantities are the main energy terms in thermal erosion. As noted in the detailed survey [22], the discharge voltage is essential for determining the spark gap size and maintaining stable discharge; the peak current determines the thermal energy applied to the workpiece surface. Also, prior experimental studies [1] have shown that power consumption and intensity are directly related to discharge current. That discharge current is the most critical factor affecting the Material Removal Rate (MRR) and several other machining parameters. In an effort to isolate their effects, both direct and through interactions, on the productivity of machining 9XC steel, the present study focused on these two fundamental energy quantities.

**Delimitations of the Experimental Range:** The operational range for the experiments was established at  $U_z = 40 - 70$  V and  $I_e = 2 - 8$  A. This particular range was chosen to simulate semi-finishing and finishing machining modes, which are important for high-hardness alloy steels that

require high precision. Specifically, the range of this operation was determined based on pilot tests and the manufacturer's instructions for the CM 323C equipment. That choice ensured stable electrical-discharge etching for 52-54 HRC steel, while still effectively balancing material removal and minimizing the risk of excessive electrode wear. The temporal parameters, pulse-on time ( $T_{on}$ ) and pulse-off time ( $T_{off}$ ), are known to influence machining results but were kept constant in this study.

While time parameters profoundly influence MRR and crater morphology by determining the duration of thermal energy application, this study proactively separates electrical parameters based on amplitude ( $U_z$  and  $I_e$ ). The  $T_{on}$  and  $T_{off}$  preserve a constant optimal value for the semi-finished regime, and the D-optimal experimental design avoids all confounding interactions between the time-pulse variation and the amplitude of the pure discharge energy. This systematic isolation is extremely important from a methodological standpoint for clearly determining the corresponding exponents of the power law. While simpler than other methods, this system is directly related to the energy strength of the hardened 9XC steel under study.

This isolation method allows for clear and simple mathematical modeling of voltage-current interactions, while remaining unaffected by pulse duration-related variables. Studies involving such variables are often incorporated into more general multiparameter studies.

### 2.3. Research Methodology

In this study, the material removal rate is denoted as  $Q$  ( $\text{mm}^3/\text{min}$ ), and the discharge current is denoted as  $I_e$  (A). The ignition voltage is denoted as  $U_z$  (V). To systematically assess the effect of voltage on the MRR of the machining tool, two-phase experiments are used in this work. Phase 1 allows a study of the separate influence of ignition voltage and discharge current ( $I_e$ ) using a One-Factor-at-a-Time method. When one parameter is varied within a limited range while the other is kept at a fixed value, and vice versa, to identify significant differences to be investigated (see Sections 3.3 and 3.4). In Phase 2, a standard  $2^2$  full factorial design is used to analyze the overall interaction of these factors. This second phase is specifically structured to generate the data necessary to build the empirical regression model (see Section 3.5 for details).

#### 2.3.1. Design of Experiments

Although techniques such as Taguchi, Response Surface Methodology (RSM), and Box-Behnken [23] are excellent for multiobjective optimization or for searching for specific optimal operating points, they are generally concerned either with quadratic approximations or with discrete-level selection to analyze process robustness. By contrast, the standard  $2^2$  full factorial design employed in this work is chosen to uniformly

cover the continuous experimental space defined by the input variables. This particular design was driven by the need to study the exponential relationship between electrical variables and performance, not local optimality search methods. Unlike the Taguchi method that seeks stability (in discrete signal-to-noise ratios) or the elaborate surface fitting of Box-Behnken and RSM, the bright orthogonal design adopted in this study guarantees that the data are robust enough to be considered dense and homogeneous to infer a continuous functional relationship. This method allows for flexible MRR prediction covering the entire voltage and current range.

#### 2.3.2. Modeling Approach

Sophisticated EDM modeling methodologies are based on either physics-based or data-driven models. For example, a thermohydraulic model based on the Finite Element Method (FEM) and Gaussian heat flux distribution has been established to predict crater shape and temperature field. Similarly, a Backpropagation (BP) Artificial Neural Network (ANN) has been used to model complex nonlinear relationships and determine optimal process parameters [24].

While these methods can provide highly accurate results in theory, they may require significant computational resources and exhibit a "black box" nature. This limits the research's ability to support rapid decision-making and directly estimate parameters for industrial users.

Empirical regression analysis is often used to develop a clear and transparent mathematical model for specific applications. This study establishes a relationship between the material removal rate ( $Q$ ) and the input parameters ( $U_z$ ,  $I_e$ ). The relationship between the parameters is then assumed to follow a power function:

$$Q = a \cdot U_z^b \cdot I_e^c \quad (1)$$

where  $a$ ,  $b$ , and  $c$  are dimensionless constants determined experimentally. These coefficients can be found using linear regression techniques. The nonlinear equation is linearized through logarithmic transformation:

$$\ln(Q) = \ln(a) + b \cdot \ln(U_z) + c \cdot \ln(I_e) \quad (2)$$

The experimental data from a  $2^2$  full factorial design can then be analyzed using the least-squares method. The method was focused on applicability, offering engineers an immediate estimate of productivity for given voltage and current settings using a simple, straightforward formula, without the need for time-consuming simulations or complex algorithm training.

### 2.4. Experimental Apparatus and Materials

To implement the experimental design and validate the regression model proposed in Section 2.3, the study was conducted on the CM 323C Electrical Discharge Machining (EDM) machine at the Mechanical Engineering Center, Hanoi University of Industry (Figure 1).



Fig. 1 CM Electrical Discharge Machining (EDM) machine

The machine’s key technical specifications, which define the operational boundaries for the selected parameters  $U_z$  and  $I_e$ , are detailed in Table 1.

Table 1. Technical specifications of the CM 323C EDM machine

Item	Specification
Machine dimensions (W×D×H)	1200×1350×2250 mm
Worktable size (W × D)	500 × 350 mm
Working range (X, Y)	300 × 200 mm
Working range (Z)	300 mm
Maximum electrode weight	60 kg
Maximum workpiece weight	500 kg
Machine weight	1000 kg
Maximum machining speed	350 mm/min

Regarding the workpiece material, consistent with the research objects defined in Section 2.1, the experiments utilized 9XC alloy tool steel. The specimens were prepared in cylindrical form ( $\text{Ø}25 \times 10 \text{ mm}$ ) and heat-treated to achieve a hardness of 52–54 HRC (Figure 2).



Fig. 2 9XC steel specimen

The specific chemical composition of the 9XC steel used in this study is presented in Table 2.

Table 2. Chemical composition of the experimental steel

Steel grade	Chemical Composition			
	%C	%Si	%Mn	%Cr
9XC	0.85-0.95	1.2 - 1.6	0.3 - 0.6	0.95 - 1.25

The machining process employed a Copper electrode with a diameter of  $\text{Ø}15 \text{ mm}$  (Figure 3) to ensure stable conductivity and thermal consistency.



Fig. 3 Copper electrode,  $\text{Ø}15 \text{ mm}$

Post-process measurements to calculate the Material Removal Rate (MRR) were performed using a high-precision Depth Micrometer (Figure 4), ensuring accurate data input for validating the mathematical model in the subsequent section.



Fig. 4 Depth micrometer

### 3. Experimental Results

#### 3.1. Modeling of the Machining Process

The experimental investigation is conceptualized as an input-output system in which machining productivity ( $Q$ ) is the primary response variable, governed by the regulation of  $U_z$  and the discharge current ( $I_e$ ). This schematic relationship, treating the EDM process as a controlled transformation unit subject to noise factors, is illustrated in (Figure 5).

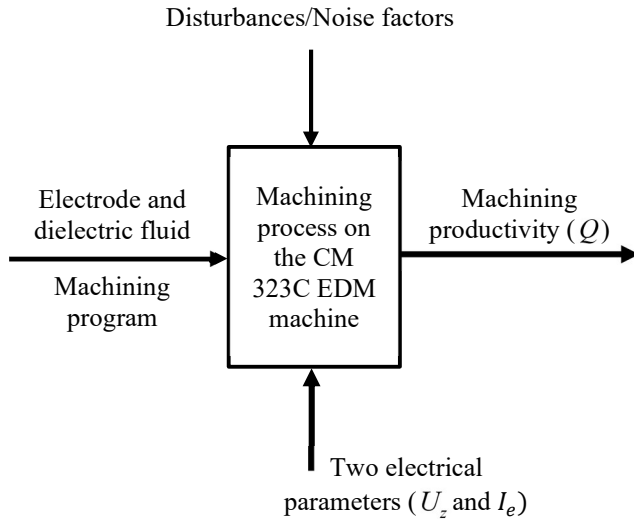


Fig. 5 Modeling of the machining process

After the experimental runs, the physical conditions in the machining zone were inspected to verify process stability. The surface conditions of the 9XC steel specimens after machining are illustrated in (Figures 6), from which the typical crater formation due to thermal erosion can be identified. (Figures 6 and 7) also show the steel and the copper electrode, confirming that the spark erosion mechanism did not change during data collection.



Fig. 6 9XC steel surface after EDM process



Fig. 7 Copper electrode surface after EDM process

### 3.2. Selection of the Number of Experiments

To determine the combined influence of  $U_z$  and  $I_e$  on machining productivity, a  $2^2$  full-factorial experimental design was used. The number of experimental runs ( $N$ ) is determined based on the number of input variables ( $k$ ) according to the following equation:

$$N = 2^k \quad (3)$$

In this study, with two input variables ( $k = 2$ ) comprising  $U_z$  and  $I_e$ , the required number of experiments is. The experimental parameters and the corresponding results, including the average response values ( $\bar{Y}_i$ ) and variances ( $S_i^2$ ) calculated from replicates, are presented in Table 3.

Table 3. Experimental parameters

N	$U_z$	$I_e$	$Y_{t1}$	$Y_{t2}$	$\bar{Y}_i$	$S_i^2$
1	40	2	90.62	90.12	90.37	0.125
2	50	4	31.30	31.50	31.40	0.020
3	60	6	21.70	21.30	21.50	0.080
4	70	8	17.50	17.84	17.67	0.060

Four experiments were performed, and results were collected with samples numbered 9 to 12. It should be noted that the sample size  $N = 4$  represents a minimal experimental dataset compared to conventional statistical designs often reported in the EDM literature, such as the Taguchi L9 or the Response Surface Method, which typically require larger experimental matrices to ensure high statistical reliability. However, the reduced dataset used in this study is considered sufficient for preliminary investigation and model validation. Each experimental run included duplicates ( $Y_{t1}$ ,  $Y_{t2}$ ) to provide the necessary degrees of freedom to estimate the net error and ensure the validity of subsequent statistical tests. However, this study is reported as a single case study testing 9XC steel at the local level. The reduced experimental matrix was selected to give a first validation of the exponential model structure and to estimate the dominant trend between voltage and current, rather than to obtain a global generalized statistical model. This approach allows for rapid decision-making in defining the relationship between electrical parameters and MRR within the specific semi-finishing regime investigated.

To ensure the reliability of this reduced dataset, the homogeneity of the experimental variances was verified using the Cochran test. The test statistic ( $G_p$ ) is calculated as the maximum variance relative to the sum of all the variances, given by:

$$G_p = \frac{\max S_i^2}{\sum S_i^2} = \frac{0.125}{(0.125+0.02+0.08+0.06)} = 0.438 \quad (4)$$

Comparing this calculated value with the critical value from the Cochran distribution table, the computed value  $G_p =$

0.438 is smaller than the critical value  $G_T = 0.684$  (with  $n=4, m=1$ ). Since  $G_p < G_T$  the experimental variances are considered homogeneous, this confirms that the experimental results are consistent and sufficiently reliable for establishing the mathematical regression model despite the small sample size.

**3.3. Effect of Ignition Voltage ( $U_z$ ) on Machining Productivity ( $Q$ )**

Machining productivity ( $Q$ ) is determined based on the volume of material removed ( $V$ ) per unit time ( $t$ ):

$$Q = \frac{V}{t} \tag{5}$$

where:

- $Q$  is the material removal rate ( $\text{mm}^3/\text{min}$ ),
- $t$  is the machining time (min),
- $V$  is the volume of material removed ( $\text{mm}^3$ ).

The volume of material removed  $V$  is determined as follows:

$$V = s \cdot h \tag{6}$$

where:

- $s$  is the discharge surface area ( $\text{mm}^2$ ),
- $h$  is the depth of the discharge crater (mm).

For the selected experimental samples, machining was performed using electrodes of identical dimensions. Therefore, the surface area and depth for all samples were the same, with:

$$s = 7.5^2 \cdot 3.14(\text{mm}^2); h = 1.0(\text{mm})$$

Thus, the volume of material removed was calculated as:

$$V = 176.625(\text{mm}^3)$$

To investigate the influence of ignition voltage on machining productivity, four experiments corresponding to four samples (No. 1 - 4) were conducted. During these experiments, all other parameters were kept constant, while only the ignition voltage was varied.

The experimental results showing the effect of ignition voltage  $U_z$  on machining productivity  $Q$  are presented in Table 4.

From Table 4, it can be observed that the influence of the ignition voltage  $U_z$  on the machining productivity  $Q$  exhibits a linear trend, since an increase in  $U_z$  the ignition voltage results in a corresponding rise in  $Q$ . Hence, the experimental correlation between the two quantities can be written in the linear form as:

$$Q = a + b \cdot U_z \tag{7}$$

**Table 4. Effect of ignition voltage  $U_z$  on machining productivity  $Q$**

Sample No.	$U_z$ (V)	$I_e$ (A)	$t$ (min)	$Q$ ( $\text{mm}^3/\text{min}$ )
1	70	6	20.17	8.75
2	60		21.50	8.21
3	50		22.45	7.86
4	40		24.07	7.33

The MATLAB programming program was used to calculate the dependence of the material removal rate on the ignition voltage (Figure 8).

Then, the machining production with ignition voltage was expressed by using Equation (8) as:

$$Q = 5.5020 + 0.0461 \cdot U_z \tag{8}$$

Typically, increasing the ignition voltage ( $U_z$ ) will increase the spark gap distance proportionally. This widened gap facilitates superior dielectric flushing, efficiently evacuating eroded debris from the machining zone and minimizing short-circuiting, thereby maintaining a highly stable material removal process.

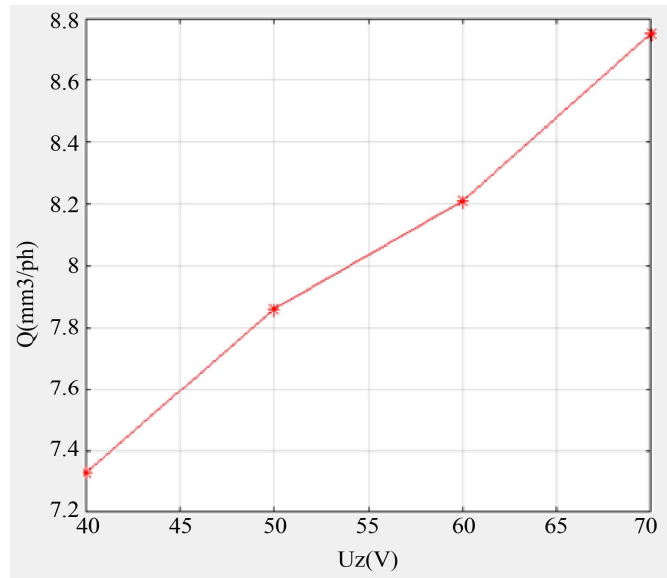


**Fig. 8 Experimental graph showing the relationship between machining productivity  $Q$  and ignition voltage  $U_z$**

**3.4. Effect of Discharge Current ( $I_e$ ) on Machining Productivity ( $Q$ )**

To investigate the effect of discharge current on machining productivity, four experiments corresponding to samples No. 5 - 8 were conducted. During these experiments, all other parameters were kept constant, while only the discharge current was varied.

The experimental results showing the influence of the discharge current  $I_e$  on machining productivity  $Q$  are presented in Table 5.

**Table 5. Effect of discharge current  $I_e$  on Machining Productivity  $Q$**

Sample No.	$U_z$ (V)	$I_e$ (A)	$t$ (min)	$Q$ (mm <sup>3</sup> /min)
5	50	8	18.5	9.55
6		6	22.0	8.03
7		4	31.4	5.63
8		2	73.2	2.41

From Table 5, it can be observed that the influence of the discharge current  $I_e$  on machining productivity  $Q$  follows a linear trend. Therefore, the empirical relationship between these two parameters can be expressed as follows:

$$Q = a + b \cdot I_e \tag{9}$$

MATLAB software was used to find and determine the relationship between machining productivity and discharge current (Figure 9).

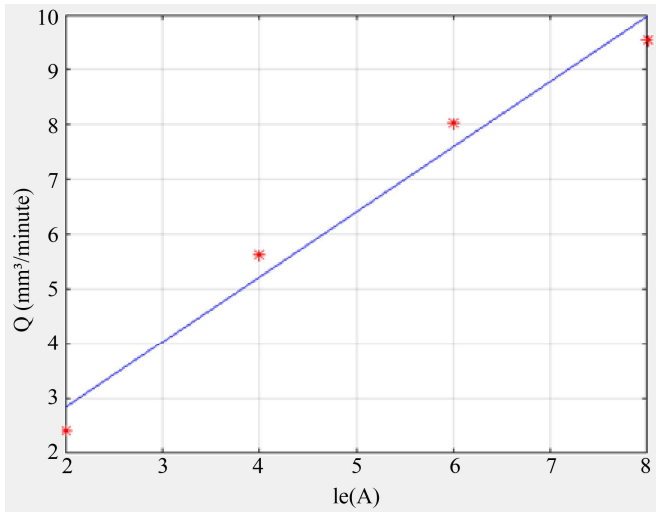


**Fig. 9** Experimental graph showing the relationship between  $Q$  and  $I_e$

Accordingly, the linear equation describing the relationship between machining productivity and discharge flow is determined using Equation (10) as follows:

$$Q = 0.45 + 1.1910 \cdot I_e \tag{10}$$

From a physical perspective, the discharge current ( $I_e$ ) directly governs the thermal energy density of the plasma channel. Higher current intensities deliver greater thermal energy to the workpiece surface, accelerating the melting and vaporization of the 9XC steel, which subsequently produces larger crater volumes and drives the linear increase in machining productivity.

### 3.5. Combined Effect of Ignition Voltage ( $U_z$ ) and Discharge Current ( $I_e$ ) on Machining Productivity ( $Q$ )

The combined influence of  $U_z$  and  $I_e$  on machining productivity ( $Q$ ) was analyzed using orthogonal experimental data. The experimental results were analyzed using regression to determine the coefficients for the power function model in Equation (1).

Accordingly, four experiments were conducted using samples numbered 9-12. All experiments were carried out using the maximum and minimum values of  $U_z$  and  $I_e$ . The experimental result is shown in Table 6.

**Table 6. Combined effect of  $U_z$  and  $I_e$  on Machining Productivity  $Q$**

Sample No.	$U_z$ (V)	$I_e$ (A)	$t$ (min)	$Q$ (mm <sup>3</sup> /min)
9	70	8	17.67	10
10	40	8	19.25	9.17
11	70	2	57.72	2.90
12	40	2	90.37	1.95

Based on previous studies, the relationship between machining productivity and the electrical parameters can be expressed in the following form, Equation (11). To apply the 2<sup>2</sup> full factorial design method, the above equation is transformed into a first-order linear multivariable form by taking the natural logarithm of both sides:

$$\ln(Q) = \ln(a) + b \cdot \ln(U_z) + c \cdot \ln(I_e) \tag{11}$$

Let:

$$y = \ln(Q); x_1 = \ln(U_z); x_2 = \ln(I_e)$$

Then, the equation becomes a first-order linear regression model:

$$y = \ln(a) + b \cdot (x_1) + c \cdot (x_2) \tag{12}$$

The logarithmic values of the experimental parameters are presented in Table 7.

**Table 7. Logarithmic values of parameters affecting Machining Productivity  $Q$**

Sample No.	$x_1 = \ln(U_z)$	$x_2 = \ln(I_e)$	$y = \ln(Q)$
9	4.248	2.079	2.303
10	3.689	2.079	2.216
11	4.248	0.693	1.065
12	3.689	0.693	0.668

The orthogonal experimental design matrix for two factors is presented in Table 8.

**Table 8. Orthogonal experimental design matrix for Q**

Sample No.	$z_1$	$z_2$	$x_1$	$x_2$	$y$
9	+ 1	+1	4.248	2.079	2.303
10	- 1	+1	3.689	2.079	2.216
11	+ 1	-1	4.248	0.693	1.065
12	- 1	-1	3.689	0.693	0.668

According to the orthogonal design method, the resulting equation has the following form:

$$y = a' + b' \cdot z_1 + c' \cdot z_2 \quad (13)$$

where the coefficients a', b', and c' are calculated as follows:

$$a' = \frac{1}{N} \sum_{i=1}^N y_i = \frac{1}{4} (2.303 + 2.216 + 1.065 + 0.668)$$

$$a' = 1.563$$

$$b' = \frac{1}{N} \sum_{i=1}^N z_{1i} y_i = \frac{1}{4} (2.303 - 2.216 + 1.065 - 0.668)$$

$$b' = 0.121$$

$$c' = \frac{1}{N} \sum_{i=1}^N z_{2i} y_i = \frac{1}{4} (2.303 + 2.216 - 1.065 - 0.668)$$

$$c' = 0.697$$

Thus, the experimental regression equation is:

$$y = 1.563 + 0.121 \cdot z_1 + 0.697 \cdot z_2$$

To transform the experimental regression equation into variables  $x_1$  and  $x_2$ , the following transformation is used:

$$z_i = \frac{x_i - \bar{x}_i}{\frac{1}{2}\Delta x_i} \quad (14)$$

where:

$\bar{x}_i$  is the mean value of  $x_i$ ,  
 $\Delta x_i$  is the range (difference) of  $x_i$ .

The regression equation was converted into variables  $x_1$  and  $x_2$  is:

$$y = -1.563 + \frac{0.121 \cdot (x_1 - 3.969)}{0.28} + \frac{0.697 \cdot (x_2 - 1.386)}{0.693}$$

$$y = -1.546 + 0.432 \cdot x_1 + 1.005 \cdot x_2$$

Therefore, the coefficients a, b, and c are obtained from Equation (11) as follows:

$$\ln(a) = -1.546 \Rightarrow a = 0.432; c = 1.005$$

Hence, the equation describing the relationship between machining productivity and ignition voltage  $U_z$ , as well as discharge current,  $I_e$  is:

$$Q = 0.213 \cdot U_z^{0.432} \cdot I_e^{1.005}$$

MATLAB software was used to plot the relationship between  $Q$  and  $U_z, I_e$ , using the following code:

```
Uz = 40 : 0.25 : 70; % declare Uz values
Ie = 2 : 0.025 : 8; % declare Ie values
[x,y] = meshgrid(Uz,Ie); % generate value matrix
Q = 0.213*(x.^0.432).*(y.^1.005);
surf(x,y,Q);
title('Effect of Uz
and Ie on Q');
xlabel('Uz (V)');
ylabel('Ie (A)');
zlabel('Q (mm^3/min)');
```

## 4. Discussion

### 4.1. Interaction Analysis and Sustainability Trade-Offs

Influence of process parameters: The power law model developed in this study ( $Q = 0.213 \cdot U_z^{0.432} \cdot I_e^{1.005}$ ) inherently includes and quantifies the nonlinear interaction between ignition voltage and discharge current. Unlike simple additive linear models, the multiplicative nature of this equation mathematically shows that the marginal effect of increasing discharge current ( $I_e$ ) on MRR is amplified syntactically at higher voltage levels ( $U_z$ ) levels. As shown in the 3D surface diagram (Figure 10), the interaction between these parameters governs the kinetics of the machining pit formation: a large discharge current provides the high heat density necessary for the melting process.

Simultaneously, a sufficiently high ignition voltage ensures a wide discharge gap. A wider gap allows for stable expansion of the plasma channel and enhances the dielectric cleaning efficiency in the molten material region, thereby limiting debris accumulation. This accumulation can hinder high-current discharge if not properly controlled.

The 3D surface plot (Figure 10) shows the relationship between machining productivity  $Q$  and the  $U_z$  and  $I_e$  as follows:

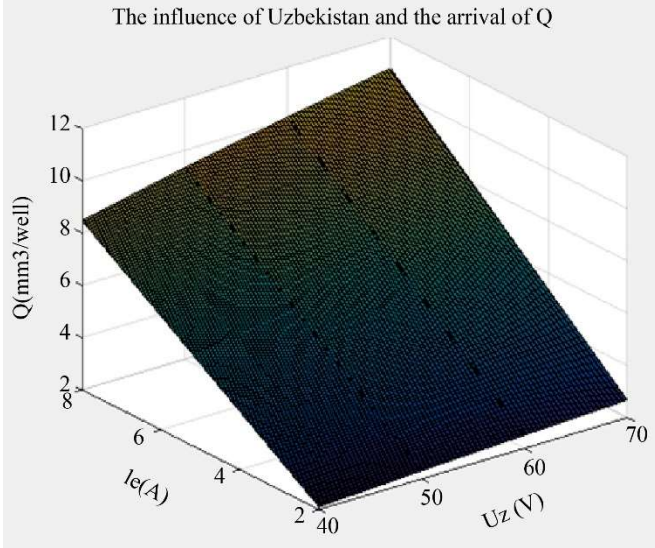


Fig. 10 3D surface plot of machining productivity Q and ignition voltage  $U_z$  and  $I_e$

Sustainability-Economic Efficiency Trade-off Analysis: The power law model was established ( $Q = 0.213 \cdot U_z^{0.432} \cdot I_e^{1.005}$ ) and serves as a quantitative basis for balancing productivity and environmental impact. While maximizing discharge current ( $I_e$ ) and ignition voltage ( $U_z$ ) significantly improves Material Removal Rate (MRR), thereby reducing machining cycle time and operating costs, it also increases specific energy consumption.

Furthermore, higher energy levels may accelerate the thermal decomposition of the dielectric fluid, thereby increasing aerosol emissions. This highlights the model's utility in multiobjective optimization to achieve a more sustainable manufacturing process for 9XC steel.

**4.2. Reliability Evaluation and Discussion**

The overall goodness and significance of the regression model is examined by the Determination Coefficient ( $R^2$ ), which is derived from the variance-based relationship:

$$R^2 = \frac{\sigma_y^2 - \sigma_{y'}^2}{\sigma_y^2} \tag{15}$$

With:

$$\begin{cases} \sigma_y^2 = \frac{1}{N-1} \cdot \sum_1^n (y_i - \bar{y}_i)^2 \\ \sigma_{y'}^2 = \frac{1}{N-1} \cdot \sum_1^n (y_i - y'_i)^2 \end{cases} \tag{16}$$

The evaluation method in this study is based on the fundamental principles of analysis of variance (ANOVA). The model's performance is then determined by comparing the explained variance with the residual variance (error), ensuring the reliability of the predicted trends.

where:

$y_i$ : experimental machining productivity ( $Q$ ),

$\bar{y}_i$ : mean value of the experimentally measured machining productivity,

$y'_i$ : predicted machining productivity obtained from the regression model,

N: number of experiments.

The calculated Coefficient of Determination for the regression model is:

$$R^2 = \frac{\sigma_y^2 - \sigma_{y'}^2}{\sigma_y^2} = \frac{0.065855 - 0.003685}{0.065855} = 0.944043$$

**4.3. Comparative Analysis and Benchmarking**

To evaluate the performance of 9XC steel within a broader industrial context, the findings of this study were benchmarked against existing literature. The dominant effect of discharge current ( $I_e$ ) over ignition voltage ( $U_z$ ) strongly aligns with the observations of Deepa et al. for carbon tool steel. However, our proposed exponential model mathematically quantifies this relationship: the exponent for current (1.005) is more than twice that for voltage (0.432) for hardened 9XC steel.

This contrasts with behaviors observed in certain composite materials where voltage plays a highly significant role (e.g., >21% contribution as reported by Mohanty). Furthermore, while recent studies have achieved high prediction accuracy using complex, computationally heavy methods like ANN or RSM [24], our straightforward exponential model yields a highly competitive reliability of 94.4%. This contrasts the model's practical superiority in that it is possible to get very precise results, and at the same time, the model is very simple and can be used in industry without a long wait.

To put the machinability of 9XC steel in perspective, the EDM performance should be compared to similar information on the commonly used mold and tool steels H13, D2, and P20 [10]. Electric Discharge Machining Current ( $I_e$ ) shares the most universally influential relationship on the Material Removal Rate (MRR) as was the case for H13 (also equivalent to SKD61/X37CrMoV5-1) and D2 (equivalent to SKD11) [8], [12].

However, since the quenched 9XC steel (52-54 HRC) is much harder than standard pre-hardened P20 steel (generally ~30 HRC), the MRR in absolute terms for 9XC is lower for the same energy inputs. Furthermore, although the exponent

in the power law model of current is approximately 1.0 for 9XC under the proposed theoretical framework, when considering materials such as D2 and H13, some differential interactions may emerge due to the presence of various complex carbides (such as chromium and molybdenum carbides) [23]. This clearly shows that although the macroscopic thermal erosion mechanism is similar for all these tool steels, the construction of specialized empirical models, such as the one proposed for 9XC in this study, is necessary to predict machining yields accurately.

## 5. Study Limitations and Future Research

Despite the meaningful findings obtained in this study, several limitations should be acknowledged. First, the experimental dataset was relatively limited, with only four experimental runs employed in the orthogonal design. Although this sample size was sufficient to establish and validate a preliminary exponential regression model, a larger dataset would enhance the model's statistical robustness and generalizability.

Second, the scope of the present investigation was deliberately restricted to two electrical parameters, namely ignition voltage ( $U_z$ ) and discharge current ( $I_e$ ), while some other significant EDM parameters, such as the pulse-on time, pulse-off time, duty cycle, and electrode wear, remained constant. Therefore, the synergistic impact of those parameters on the machining performance was not investigated.

Third, the surface roughness was measured at the experiments, but no in-depth study of the microstructure of machined surfaces, with SEM observation and recast layer examination, was performed. These types of analysis would allow a better understanding of the process of material removal as well as the surface integrity under various electrical regimes.

Future research should, therefore, aim at extending the experimental design by introducing more temporal parameters into bigger statistical matrices like Taguchi or RSM. Most significantly, the explicit empirical regression model developed in this basic study will directly act as an essential quantitative baseline common to future studies involving advanced hybrid processes, namely Powder-Mixed EDM (PMEDM) and Ultrasonic-Assisted EDM (UAEDM).

The analysis of the systematic changes induced by the influences of acoustic cavitation dynamics (or conductive dielectric powder EC), in the mathematical coefficients and exponents of the proposed power-law function, will provide profound insights for the development of intelligent

manufacturing and precision machining of 9XC alloy tool steel. At the end, considering economic and environmental effects, on the one hand, maximizing MRR reduces active machining time, leading to a reduction of total energy consumption and machining depreciation cost.

On the other hand, the environmental effect of aerosol emissions of traditional hydrocarbon-based dielectrics is a matter of concern. In future work, the trade-offs between machining cost, tool wear rate, and carbon emissions need to be holistically analyzed. Integrating environmentally friendly options, such as water-based or vegetable oil-based dielectrics, into this optimization framework would be a crucial step toward a fully sustainable EDM machining process.

## 6. Conclusion

From the research results, experiments, and data processing, the mathematical relationship between ignition voltage and machining productivity has been determined as  $Q = 5.5020 + 0.0461 \cdot U_z$ . A formula for the discharge current as a function of the machining productivity is given by  $Q = 0.45 + 1.1910 \cdot I_e$ . In addition, the combined effect of the ignition voltage  $U_z$  and discharge current  $I_e$  on machining productivity was expressed by the following equation  $Q = 0.213 \cdot U_z^{0.432} \cdot I_e^{1.005}$ .

The proposed model demonstrated high reliability with a Coefficient of Determination ( $R^2$ ) of 0.944. Furthermore, comparative benchmarking confirms that 9XC steel exhibits distinct machining characteristics compared to standard H13 and D2 steels, underscoring the need for the proposed material-specific empirical model for precision toolmaking. Discharge current ( $I_e$ ) has a substantially greater influence on machining productivity than ignition voltage ( $U_z$ ), as indicated by the regression model exponents (1.005 vs 0.432).

The results of this study provide a basis for process engineers to calculate and select appropriate machining parameters, thereby improving productivity and surface quality when machining 9XC steel on the CM 323C electrical discharge machining machine, in particular, and serving as a reference for selecting suitable machining conditions in EDM processes in general.

## Funding Statement

The author is responsible for all research work, including the fabrication of the material and the writing of the thesis. The author has not received financial assistance from any external body or organization.

## References

- [1] André F. V. Pedroso et al., “Electrical Discharge Machining of Composites: A Critical Review of Challenges and Innovations,” *Journal of Mechanical Engineering and Manufacturing*, vol. 1, no. 1, pp. 1-20, 2025. [[CrossRef](#)] [[Google Scholar](#)] [[Publisher Link](#)]
- [2] Linun Liu et al., “Optimization of Wire EDM Process Parameters on Cutting Inconel 718 Alloy with Zinc-Diffused Coating Brass Wire Electrode Using Taguchi-DEAR Technique,” *Coatings*, vol. 12, no. 11, pp. 1-13, 2022. [[CrossRef](#)] [[Google Scholar](#)] [[Publisher Link](#)]
- [3] Anand Pandey, and Shankar Singh, “Current Research Trends in Variants of Electrical Discharge Machining: A Review,” *International Journal of Engineering Science and Technology*, vol. 2, no. 6, pp. 2172-2191, 2010. [[Google Scholar](#)]
- [4] M. Kunieda et al., “Advancing EDM through Fundamental Insight into the Process,” *CIRP Annals*, vol. 54, no. 2, pp. 64-87, 2005. [[CrossRef](#)] [[Google Scholar](#)] [[Publisher Link](#)]
- [5] Hassan Abdel-Gawad El-Hofy, *Advanced Machining Processes, Nontraditional and Hybrid Machining Processes*, McGraw Hill, pp. 1-288, 2005. [[Google Scholar](#)] [[Publisher Link](#)]
- [6] Thuy Duong Nguyen, Khanh Huyen Nguyen, and Long Nguyen Ha, “A Comparison of RSM-DA and PSO-TOPSIS in Optimizing the Finishing Turning of 9XC Steel under MQL Conditions,” *Engineering, Technology & Applied Science Research*, vol. 14, no. 3, pp. 14044-14048, 2024. [[CrossRef](#)] [[Google Scholar](#)] [[Publisher Link](#)]
- [7] Nguyen Truong Giang, Do Manh Tung, and Le Van Tao, “Optimizing the Tool Wear Rate When Machining 9XC Steel in the EDM Process Mixing Tungsten Compound Powder by Desirability Approach Method,” *International Research Journal of Advanced Engineering and Science*, vol. 9, no. 1, pp. 123-127, 2024. [[Google Scholar](#)] [[Publisher Link](#)]
- [8] Kapil Surani et al., “Optimization of EDM Parameters for Enhanced Machining of X37CrMoV5-1 Tool Steel using Taguchi Method and Regression Analysis,” *Scientific Reports*, vol. 15, pp. 1-17, 2025. [[CrossRef](#)] [[Google Scholar](#)] [[Publisher Link](#)]
- [9] P. Janagarathinam et al., “Investigation of Machining Rate and Surface Roughness in wire EDM of Al6063/WC/ZrO2 Composite Using Response Surface Methodology,” *Materials Research Express*, vol. 11, no. 2, pp. 1-19, 2024. [[CrossRef](#)] [[Google Scholar](#)] [[Publisher Link](#)]
- [10] Van-Tao Le et al., “Modeling, Impact Evaluation, and Optimization of Machining Performances of Heat-Treated SKD61 Steel in a Tungsten Powder Alloy Mixed EDM Process via the RSM-GRA Methodology,” *Science and Technology Development*, vol. 26, no. 4, pp. 3150-3160, 2023. [[CrossRef](#)] [[Google Scholar](#)] [[Publisher Link](#)]
- [11] Deepa Singh et al., “Analysis of EDM Process Parameters for Maximizing Material Removal Rate in SK2Mcr4 Steel Machining,” *Journal of Materials and Environmental Science*, vol. 16, no. 6, pp. 950-967, 2025. [[Google Scholar](#)] [[Publisher Link](#)]
- [12] Devendra Pendokhare et al., “A Comprehensive Review of Parametric Optimization of Electrical Discharge Machining Processes using Multi-Criteria Decision-Making Techniques,” *Frontiers in Mechanical Engineering*, vol. 10, pp. 1-26, 2024. [[CrossRef](#)] [[Google Scholar](#)] [[Publisher Link](#)]
- [13] Muhamad Taufik Ulhakim et al., “Electrical Discharge Machining: Recent Advances and Future Trends in Modeling, Optimization, and Sustainability,” *International Journal of Lightweight Materials and Manufacture*, vol. 8, no. 4, pp. 495-511, 2025. [[CrossRef](#)] [[Google Scholar](#)] [[Publisher Link](#)]
- [14] S. Tripathy, and D. K. Tripathy, “Multi-Response Optimization of Machining Process Parameters for Powder Mixed Electro-Discharge Machining of H-11 Die Steel using Grey Relational Analysis and Topsis,” *Machining Science and Technology*, vol. 21, no. 3, pp. 362-384, 2017. [[CrossRef](#)] [[Google Scholar](#)] [[Publisher Link](#)]
- [15] Md Ehsan Asgar, Ajay Kumar Singh Singholi, “A Review on Wire Electrical Discharge Machining of Advanced Conductive Materials,” *International Transaction Journal of Engineering*, vol. 12, no. 10, pp. 1-10, 2021. [[CrossRef](#)] [[Google Scholar](#)] [[Publisher Link](#)]
- [16] Vijaykumar S. Jatti et al., “Machine Learning Based Predictive Modeling of Electrical Discharge Machining of Cryo-Treated NiTi, NiCu and BeCu Alloys,” *Applied System Innovation*, vol. 5, no. 6, pp. 1-11, 2022. [[CrossRef](#)] [[Google Scholar](#)] [[Publisher Link](#)]
- [17] Piotr Myśliwiec, and Andrzej Kubit, “Integrated Multiobjective Optimization of RFSSW Parameters for AA2024-T3 using ANOVA Machine Learning and NSGA II,” *Scientific Reports*, vol. 15, pp. 1-23, 2025. [[CrossRef](#)] [[Google Scholar](#)] [[Publisher Link](#)]
- [18] Prabhu Loganathan et al., “Optimization of Electrochemical Machining Process Parameters using Artificial Neural Network,” *International Conference On Modelling Strategies In Mathematics*, Coimbatore, India, 2025. [[CrossRef](#)] [[Google Scholar](#)] [[Publisher Link](#)]
- [19] Dauglas C. Montgomery, *Design and Analysis of Experiments*, 9<sup>th</sup> ed., John Wiley & Sons, pp. 1-752, 2020. [[Google Scholar](#)] [[Publisher Link](#)]
- [20] Amandeep Singh Bhui et al., “Experimental Investigation of Optimal Ed Machining Parameters for Ti-6Al-4V Biomaterial,” *Facta Universitatis, Series: Mechanical Engineering*, vol. 16, no. 3, pp. 337-345, 2018. [[CrossRef](#)] [[Google Scholar](#)] [[Publisher Link](#)]
- [21] Van Tung Nguyen et al., “Determination of Best Input Factors in Powder-Mixed Electrical Discharge Machining 90CrSi Steel using Multi-Criteria Decision Making Methods,” *Engineering, Technology and Applied Science Research*, vol. 15, no. 1, pp. 19121-19127, 2025. [[CrossRef](#)] [[Google Scholar](#)] [[Publisher Link](#)]
- [22] Jaber E. Abu Qudeiri et al., “Advanced Electric Discharge Machining of Stainless Steels: Assessment of the State of the Art, Gaps and Future Prospect,” *Materials*, vol. 12, no. 6, pp. 1-48, 2019. [[CrossRef](#)] [[Google Scholar](#)] [[Publisher Link](#)]

- [23] Van-Canh Nguyen et al., "Toward Sustainable Machining of Hardened SKD11: Machine Learning-Based Evaluation and Optimization of Surface Roughness, Tool Wear, and CO<sub>2</sub> Emissions," *Results in Engineering*, vol. 26, pp. 1-17, 2025. [[CrossRef](#)] [[Google Scholar](#)] [[Publisher Link](#)]
- [24] V.N.R. Jampana, P.S.V. Ramana Rao, and A. Sampathkumar, "[Retracted] Experimental and Thermal Investigation on Powder Mixed EDM Using FEM and Artificial Neural Networks," *Advances in Materials Science and Engineering*, vol. 2023, no. 1, 2023. [[CrossRef](#)] [[Google Scholar](#)] [[Publisher Link](#)]